Chimica Techno Acta
published by Ural Federal University
eISSN 2411-1414
chimicatechnoacta.ru

ARTICLE
2024, vol. 11(2), No. 202411201
DOI: 10.15826/chimtech.2024.11.2.01

Effects of coagulant bath temperature toward separation performance and antifouling properties of PVDF/CA membranes for filtration of dyes

Muhammad Reza [a], Ratu Fazlia Inda Rahmayani [b]*, Cynthia Linaya Radiman [c]

a: Chemical Education Study Program, Universitas Islam Negeri Ar-Raniry, Banda Aceh 23111, Indonesia
b: Department of Chemistry Education, Universitas Syiah Kuala, Banda Aceh 23111, Indonesia
c: Inorganic and Physical Chemistry Division, Institut Teknologi Bandung, Bandung 40116, Indonesia
* Corresponding author: ratu_fazlia@usk.ac.id

This paper belongs to a Regular Issue.

Abstract

Phase inversion is used to prepare poly(vinylidene fluoride) (PVDF) microfiltration membranes by combining it with the hydrophilic polymer additive cellulose acetate (CA). For the filtration of methylene blue (MB) and acid yellow 17 (AY17), the effects of coagulant bath temperature (CBT) on the separation performance and antifouling properties are thoroughly investigated. SEM analysis shows that the membrane at higher CBT has a larger pore diameter than at lower CBT, resulting in differences in membrane surface hydrophilicity. It is found that the increase in surface hydrophilicity causes the permeability of PVDF/CA membranes to be higher at higher CBT than at lower CBT. Rejection values above 90% indicate that the membranes are more effective for MB separation at both lower and higher CBT. Otherwise, lower CBT provides better AC rejection than higher CBT. The Flux Recovery Ratio, which is higher at higher CBT, remains in the 75–95% range at lower CBT. As a result, lower CBT is better for membrane fouling resistance than higher CBT. In addition, the fouling observed at lower CBT is similar to the fouling observed at higher CBT, but lower CBT has a higher percentage of reversible fouling than higher CBT. The membranes with more reversible fouling are therefore easier to clean using the backwashing process. As a result, PVDF/CA membranes manufactured at lower CBT have better separation performance and antifouling characteristics than those manufactured at higher CBT.

Keywords

poly(vinylidene) fluoride
coagulant bath temperature
flux recovery ratio
antifouling properties
methylene blue
acid yellow 17

Received: 23.02.24
Revised: 21.03.24
Accepted: 27.03.24
Available online: 01.04.24

Key findings

- PVDF/CA membranes fabricated using different coagulant bath temperatures show different separation performance.
- The membranes with a lower CBT exhibit greater selectivity for the separation of both dyes, MB and AC, as indicated by rejection rates exceeding 90%.
- Although the membranes on the higher and lower CBT have almost identical total fouling, the membrane on the lower CBT has more reversible fouling.

1. Introduction

Membrane technology plays a crucial role in the chemical industry. Its versatility is demonstrated by the numerous applications of membranes, including the creation of clean water, the reduction of pollution levels, the removal of harmful elements, and the separation of specific chemicals from industrial wastes [1]. This technology is popular due to its high efficiency for separation, low energy consumption, usability, and ability to be used in soft systems [2, 3].

Poly(vinylidene fluoride) (PVDF) is reported to be one of the most widely used polymeric materials as a membrane material in recent years. Due to its semi-crystalline structure, PVDF has excellent thermal, chemical and mechanical properties [4-6]. Because of these good properties, PVDF is widely used for various applications such as microfiltration [7], ultrafiltration [8], pervaporation [9], membrane distillation [10, 11] and gas-liquid membrane contactors [12].

In the manufacture of ultrafiltration membranes, these membranes are usually produced by a non-solvent-induced phase separation (NIPS) technique [13]. In this process, the casting solution contains a mixture of polymer and solvent (with or without additives), which is then immersed in a coagulant bath containing a non-solvent, usually water. As PVDF is hydrophobic, the penetration of the coagulant (water) into the polymer casting solution is limited during the phase inversion process [14]. It will therefore be a challenge to create the pores in the membrane. To prepare for this, chemicals that can act as pore-forming agents must be applied to the PVDF membrane. In contrast to PVDF, which is hydrophobic, additives with different properties are typically used, such as CA, which is hydrophilic. In this process, hydrophilic PVDF is created by blending a variety of hydrophilic polymers, including CA, amphiphilic block copolymers and inorganic nanoparticles [5,15]. Due to this miscibility, the casting solution is thermodynamically completely separated during the phase inversion process. As a result, many pores can be created due to the large number of additives that come out of the casting solution into the coagulant (water) [12].

During the production of PVDF membranes from casting solutions, a thermodynamic and kinetic nonequilibrium process takes place. This process is influenced by various factors, such as solvents, non-solvents, additives, the composition of the coagulant bath, and the viscosity of the casting solutions [16-18]. The coagulant bath temperature (CBT) has a significant impact on this nonequilibrium process, which affects both the phase separation process and the performance of the membrane [19-22]. During phase inversion, the concentration of polymer decreases in the polymer-rich phase and increases in the less polymeric phase, resulting in a looser membrane. The solubility increases with the high temperature of CBT, leading to a faster diffusion rate of solvent and non-solvent and an accelerated phase inversion process. Therefore, membranes produced at higher CBT are more likely to have a thinner surface layer and be more porous [20, 22, 23].

The performance of the membrane will deteriorate due to fouling that occurs over time during dye microfiltration. Typically, a hydrophilic homopolymer solution containing additives such as poly(ether glycol) (PEG), poly(vinylpyrrolidone) (PVP), and cellulose acetate (CA) is used to prevent fouling on PVDF membranes. Hydrophilic chemicals are added to create pores or increase porosity, as well as to prevent fouling. Previous studies have shown that PVDF membranes blended with CA are effective for BSA separation [24]. PVDF/CA membranes have also been tested for methylene blue (MB) filtration, and they have demonstrated improved antifouling properties with reversible fouling up to 55% [25]. Additionally, the separation performance of PVDF membranes can vary depending on the CBT temperature used in their production, as shown in other studies. The study investigated the effect of CBT on the performance of the PVDF/Pluronic F127 blend membrane. The best performance was observed at higher CBT [26]. It was found that CBT influences antifoulings, with higher CBT resulting in reduced membrane antifouling properties [13]. Therefore, the membranes were fabricated at lower CBT to assess the influence of CBT on changes in the antifouling properties of the PVDF/CA membranes. The study investigated the impact of CBT variation on the performance of PVDF/CA membranes in microfiltration of Methylene Blue (MB) and Acid Yellow 17 (AY17).

2. Experimental

2.1. Materials

Poly (vinylidene fluoride) (PVDF) powder (Solef® 1015) was distributed by Solvay. Cellulose acetate (CA) (MW = 30,000 Da) was supplied by Sigma Aldrich. N,N-dimethylacetamide (DMAc) (99%, Merck) was used as a solvent. Then, it used distilled water as nonsolvent in a coagulant bath. Sulfuric acid (H_2SO_4) (95–97%, Merck) was obtained from Singapore. Methylene blue ($C_{16}H_{18}ClN_3S{\cdot}xH_2O$, 319.85 g/mol, Merck) and Acid Yellow 17 ($C_{16}H_{10}Cl_2Na_2O_7S_2$, 551.29 g/mol) were used for dye microfiltration.

2.2. Membrane fabrication

The PVDF/CA blend membranes were fabricated using the phase inversion method. Initially, PVDF and CA were mixed in DMAc at 60 °C with various concentration ratios as presented in Table 1. The mixture was stirred for 24 h to ensure the polymers were thoroughly mixed. To remove any trapped bubbles in the mixture, the removal process was carried out for 4 h without stirring. Afterwards, the solutions were poured onto a glass plate and immediately placed in a coagulant bath at temperatures of 10 °C using a cold coagulant bath and 25 °C at room temperature. The resulting membranes were washed thoroughly with deionised water to remove any residual solvent and then stored in water before being used for microfiltration.

Table 1 Dope composition of PVDF/CA membranes.

Membranes	Polymer (18 wt.%)		Solvent, DMAc (wt.%)
	PVDF	CA	
PVDF	100	0	82
M1	99	1	82
M2	97	3	82
M3	95	5	82
M4	90	10	82
M5	80	20	82

 DOI: 10.15826/chimtech.2024.11.2.01

2.3. Microfiltration experiments

The permeability properties of the membranes were evaluated using a filtration method in a dead-end microfiltration cell. Each membrane was compacted at 2 bars by passing distilled water for 30 min. The water flux (J_w) was calculated using Equation 1 [27], where V is the volume of collected permeate, A is the membrane area, and t is the permeation time.

$$J_w = V/(A \cdot t) \quad (1)$$

To determine the antifouling properties, dye filtration was performed using 1000 ppm methylene blue and acid yellow 17 solutions under 2 bars for 30 min and the flux of the dye solutions was recorded as J_p. The membranes were then immersed in deionised water for 5 min before being used for backwash treatment to calculate the flux ratio recovery (FRR). The percentage of FRR of the membranes was determined using equation 2 [27, 28], where J_R is the recovery flux of the membranes after filtration with dye solution and J_w is the water flux during the densification period.

$$\mathrm{FRR} = (J_R/J_w)\, x\, 100\% \quad (2)$$

The membrane's selectivity towards dyes was measured as a percentage of rejection. The concentrations of the permeate and concentrated solutions were calculated using linear equations of standard solutions with five concentration variations. The absorption of the solutions was determined using a UV-visible spectrophotometer (EVOLUTION 220). The permeate solutions were collected after the microfiltration tests. The analysis of methylene blue (MB) solutions was conducted at 665 nm [29], while the analysis of acid yellow 17 was measured at 418 nm [30].The rejection (R), total fouling ratio (R_t), reversible fouling ratio (R_r), and irreversible fouling ratio (R_{ir}) were calculated using Equations 3–6 [17].

$$R = (C_0 - C_1)C_0 \cdot 100\%, \quad (3)$$

$$R_t = (J_w - J_P)J_w \cdot 100\%, \quad (4)$$

$$R_r = (J_R - J_P)J_w \cdot 100\%, \quad (5)$$

$$R_{ir} = (J_w - J_R)J_w \cdot 100\%. \quad (6)$$

The surface hydrophilicity of the membranes was measured using a water contact angle meter (θ). The membrane sheet was placed on a sample holder and deionized water was dropped onto the surface using a Mitutoyo sessile drop. The Gibbs free energy of hydration (ΔG_{SW}) of membranes was calculated using Young-Dupré Equation 7 [31, 32], where θ represents the average contact angle and γ_w represents the water surface tension (72.8 mJ m^{-2} for deionized water at room temperature).

$$-\Delta G_{SW} = (1 + \cos\theta)\gamma_w \quad (7)$$

3. Results and Discussion

3.1. Effect of CBT on water flux of PVDF/CA membranes

Permeability and selectivity are important factors in membrane separation performance. To evaluate both of these factors, microfiltration of dyes is used. Membrane permeability is measured by water flux, while selectivity is measured by rejection (as discussed further in Section 3.3). Figure 1 illustrates the effect of CBT on membrane water fluxes. The M3 membrane demonstrated the highest water flux at both 10 and 25 °C when treated with CBT. The optimal composition of the PVDF/CA blended membrane is achieved by adding 5% weight of CA. The water fluxes of the membranes manufactured at 10 and 25 °C demonstrate the impact of CBT on performance, with all membranes cast at CBT 25 °C achieving higher fluxes than those cast at CBT 10 °C.

The phase inversion approach is employed in the fabrication of membranes at two different temperatures: 25 °C at room temperature and 10 °C to investigate the results below room temperature. According to a previous study, increasing the thermodynamic stability of the dope polymer solution causes the inversion rate to deteriorate [33–35]. This is slow down the rate of phase inversion, causing the polymer precipitation to form gradually. The slow precipitation delays the phase separation process and increases the contact between the dope solution and the water used as a coagulant bath. This interaction results in macrovoids with shorter and narrower pores, constructed at a lower CBT [26], as shown in Figure 2.

Figure 1 demonstrates that the membranes produced at higher CBT exhibit greater permeability to water than those produced at lower CBT. However, the trend of water flux across membranes at higher CBT is similar to that at lower CBT, indicating that the composition of PVDF/CA was not affected by the CBT. The composite PVDF/CA membranes outperformed PVDF membranes in terms of water filtration permeability.

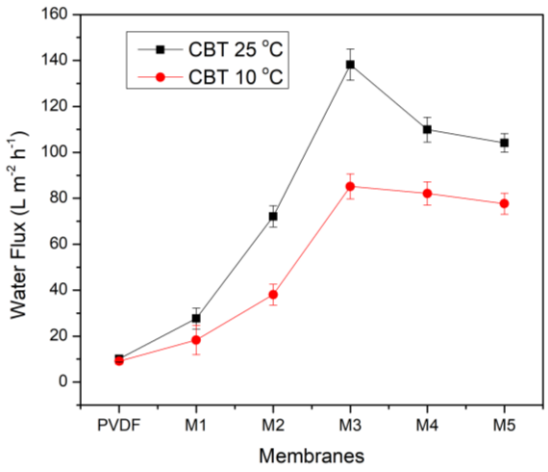

Figure 1 Effect of CBT on membrane water flux.

 DOI: 10.15826/chimtech.2024.11.2.01

The only information provided with the results was the rate of different phase inversions affected by different CBTs. As the CBT represents both thermodynamic and kinetic factors in the phase inversion process [19-23], the study of thermodynamics is particularly necessary. By measuring the water contact angle, the Gibbs free energy of hydration can be calculated. The ideal water flux value, denoted by M3, indicated the ideal composition. Therefore, the following measurement only allowed for M3 in the composition.

3.2. Effect of CBT on the hydrophilicity properties of PVDF/CA membrane surface

The hydrophilicity of a membrane can be characterised by measuring the water contact angle. In addition, these properties can also be demonstrated by calculating the Gibbs free energy of hydration ($-\Delta G_{sw}$). The results of the contact angle and Gibbs free energy of hydration measurements are shown in Figure 3. Figure 3a shows that the addition of CA composition decreases the contact angle, namely 72.93°, 60.87° and 56.43 for M1, M2 and M3 respectively. The decrease in contact angle indicates an increase in surface hydrophilicity. The membrane surface becomes more hydrophilic with the addition of CA. Considering that CA is very hydrophilic and the addition of hydrophilic substances to PVDF will significantly increase the surface hydrophilicity of the membrane [36, 37]. Furthermore, it can be seen that the $-\Delta G_{sw}$ value is higher for composite membranes than for PVDF. The $-\Delta G_{sw}$ value increased by 26.4% from PVDF to the highest value of M3. Figure 3b shows the decrease in contact angle which is not significant. That is, the contact angle decreases by only 13.79% on M3 compared to PVDF membranes. Furthermore, the higher the CBT, the lower the Gibbs free energy, indicating a stronger interaction between CA and non-solvent during phase inversion, resulting in more CA leaving the dope solution and forming pores. Conversely, a lower CBT reduces the interaction of CA with water as a non-solvent, resulting in fewer surface pores (Figure 4).

Depending on the application, the membrane is manufactured with a specific CA composition, so measuring the water contact angle is critical. Membranes with a contact angle between 0 and 90° are considered hydrophilic, whereas those with a contact angle of 90° or more are considered hydrophobic.

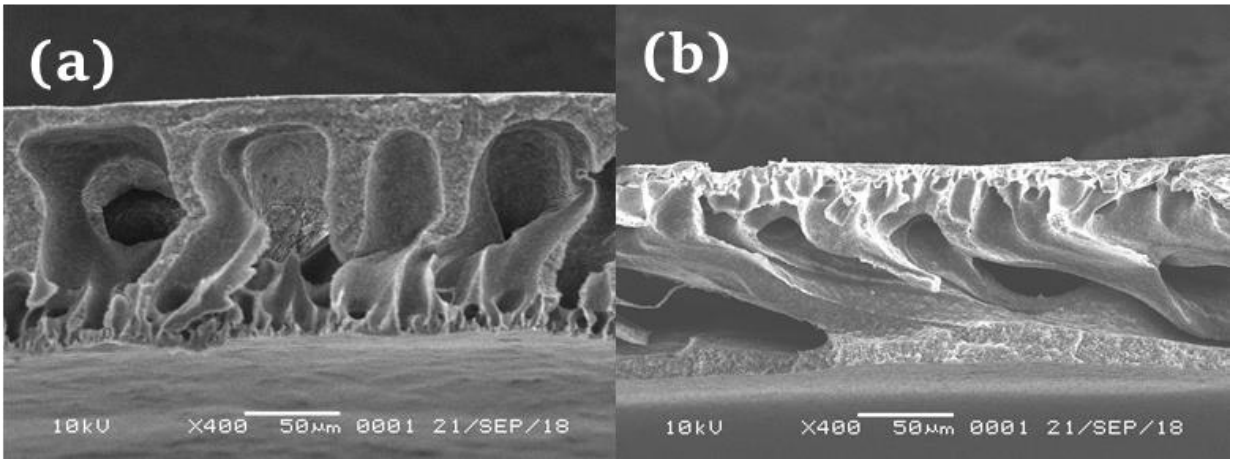

Figure 2 Effect of CBT 25 °C (a) and 10 °C (b) on macrovoids profile of M3 membrane.

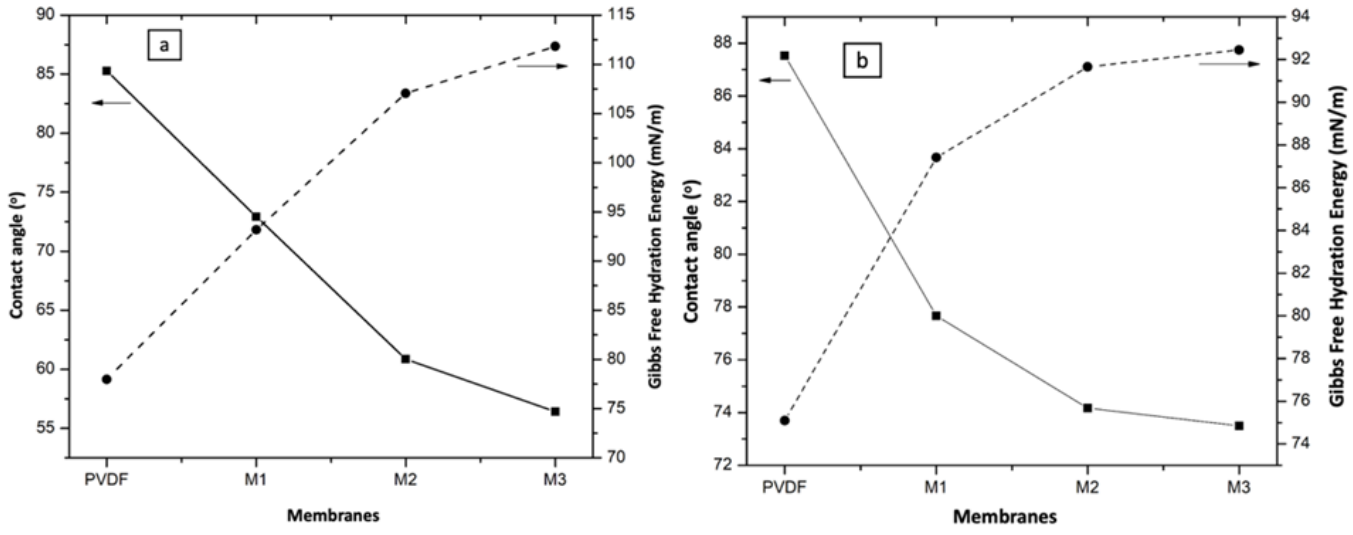

Figure 3 Effect of CBT 25 °C (a) and 10 °C (b) on water contact angle and Gibbs free hydration energy.

 DOI: 10.15826/chimtech.2024.11.2.01

Membranes with a contact angle of 150° are considered superhydrophobic [38]. All membranes have water contact angles below 90° as shown in Figure 3, indicating that the membranes have hydrophilic surfaces. In accordance with the ideal water flux, the M3 membrane had the lowest water contact angle, indicating that its surface is more hydrophilic than that of the other membranes. A higher CBT results in a larger water contact angle than a lower CBT at different CBTs. This result is consistent with previous research showing that CBT and water contact angle both improve [13, 26]. In addition, this result is influenced by the greater surface hydrophilicity of the membranes at higher CBT than at lower CBT. The different surface profile is further supported by the SEM image shown in Figure 4. The diameter of the pores in the M3 membrane produced on CBT 10 °C is significantly different from that of CBT 25 °C.

The Gibbs free energy of hydration, which can be calculated thermodynamically to determine how much energy the system produces during the hydration process, is shown in Figure 3. The Gibbs free energy is released in proportion to the amount of water taken up by the membrane surfaces. Because the system has been given the work done by the water system at the membrane surface, energy is released. In addition, the Gibbs free energy of hydration is a function of the water contact angle [39]. At different CBTs, the higher CBT results in a higher Gibbs free energy of hydration than at lower CBTs. This shows that the surface of the composite membrane can interact more easily with water. The higher Gibbs free energy of hydration results in the longest wetting time [37].

The dynamic contact angle is the next characterization to assess the hydrophilicity of the membrane surface. The decrease in the dynamic contact angle corresponds to a change in the number of polymorphic beta fractions in the membranes [40]. The presence of the CA component also results in an increase in the polymorphic beta fractions, causing the contact angle to decrease faster than that of the pure PVDF membrane. Figure 5 shows the results of this measurement. Over 30 minutes, the contact angle decreased similarly for all membranes. M3 had the lowest contact angle of 20.67° at 30 min compared to the other membranes. The contact angle in the CBT membrane conditions did not decrease significantly; it was maintained above 60° after 30 min. After 20 min, M2 showed a sharp decrease, while the contact angle of M3 showed the same after 15 min.

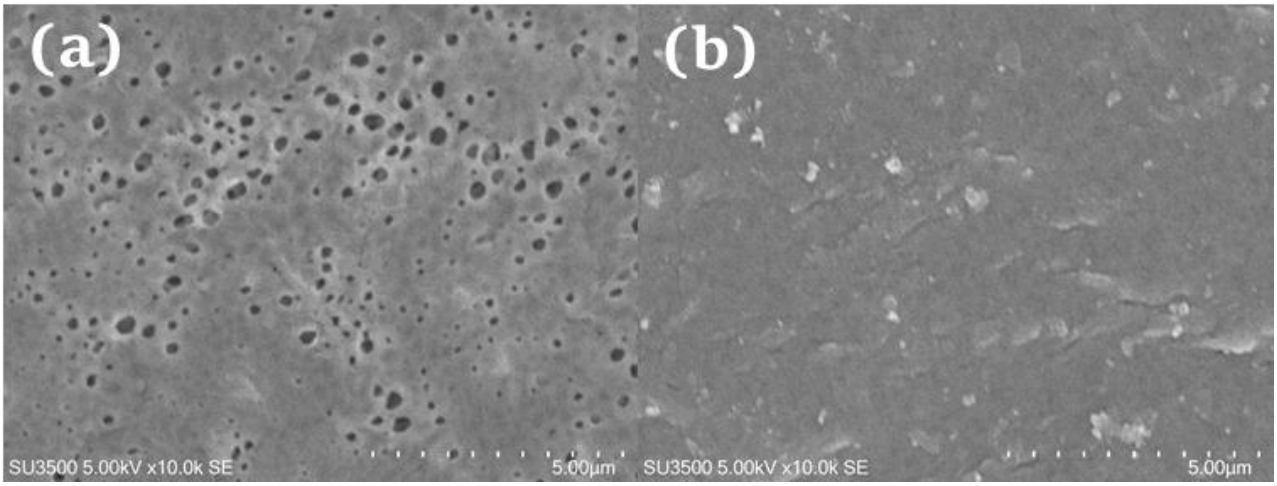

Figure 4 Effect of CBT 25 °C (a) and 10 °C (b) on pore diameter of M3 membrane surface.

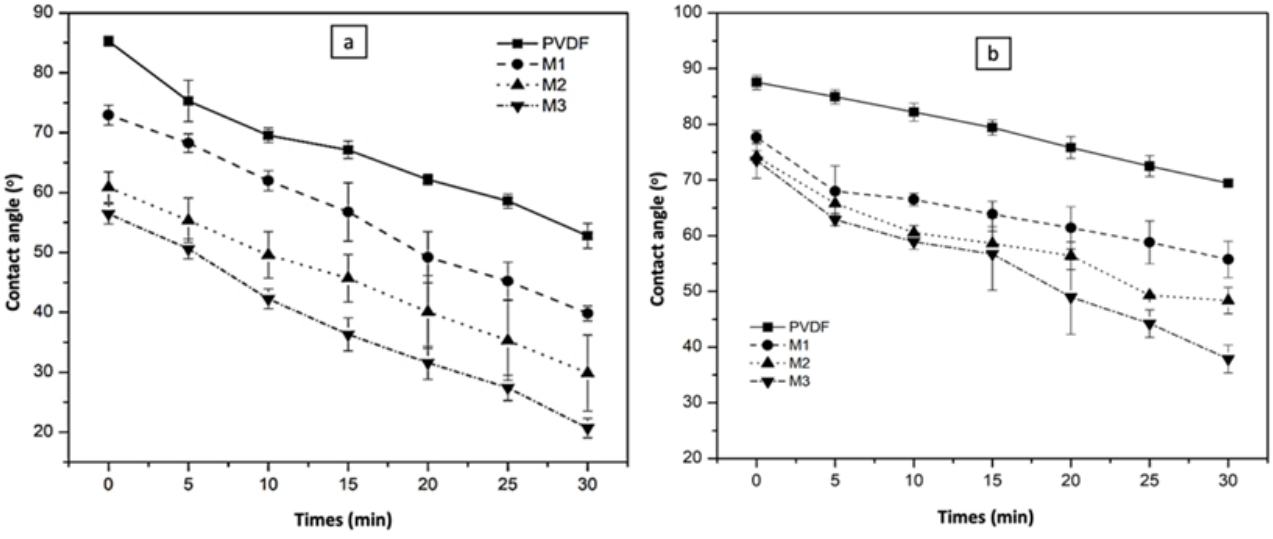

Figure 5 Effect of CBT 25 °C (a) and 10 °C (b) on membrane surface hydrophilicity.

 DOI: 10.15826/chimtech.2024.11.2.01

The hydration process is spontaneous if the Gibbs free energy of hydration value is always negative. In this experiment, the dynamic contact angle measurement is performed for 30 min, while the contact angle is measured every 5 min to empirically demonstrate the spontaneous process. The results of previous experiments have shown that modified PVDF membranes have a significant effect on the contact angle [41]. The water contact angle continues to decrease every 5 min, Figure 5. This means that water continues to be spontaneously absorbed into the membrane pores through the surface [42]. In addition, the M3 membrane reduces the water angle more than other membranes because its surface is more hydrophilic. The numerous distinct decreases in contact angle at lower CBT demonstrate the effect of different CBTs on this property. The surface modification, such as increased hydrophilicity, will differentiate the contact angle [43] and influence the interaction between water and the membrane surface.

3.3. Effect of CBT on separation performance of PVDF/CA membranes

The percentage of rejection (%*R*), flux recovery ratio (%FRR), and antifouling properties are used to evaluate separation performance. Figure 6 illustrates how well membranes separate dyes during filtration. In general, the membranes are more effective at removing MB than AY17. Figure 6a shows that for each membrane at both the lower and higher CBT, the rejection of methylene blue (MB) was greater than 90%. However, the rejection of AY17 is only effective at the lower CBT, as indicated by the rejection percentage of M1 being above 90, while the remaining percentage remained above 80%. In addition, the rejection of less than 90% indicated that the membranes produced at higher CBT were poor at separating AC. As shown in Figure 1, the addition of 5% CA significantly increased the permeability. A previous study showed that even with the addition of 5% CA, the rejection of PVDF/CA membranes against MB can reach 97% [25]. Similarly, Figure 6 further shows that the additional 5% CA maintains the rejection rate above 94% against MB.

Rejection is a method of measuring the selectivity of a membrane. The percentage of rejection is used to express the rejection. When the rejection percentage is at least 90%, the membranes have good selectivity according to experimental data. However, because the pore diameter on the surface is not homogeneous (Figure 4), only a small number of dyes are absorbed. For example, at lower and higher CBT, the M3 membrane rejects 94% and 91% of the MB, respectively. This indicates that the filtration process still removed 210% of the MB present in the water.

When the MB rejection is compared to the AY17 rejection, the MB rejection is above 90% for both the lower and higher CBT. Only the M1 membrane at the lower CBT has an AY17 rejection above 90%; the rest are below 90%. In other words, PVDF/CA membranes are more useful for MB rejection than AY17 because they have better membrane selectivity towards MB. The surface charge of PVDF membrane tends to be negative [44], and the addition of CA during the mixing process successfully enhances the negative charge of the surface. MB is a cationic dye, while AY17 is a negative dye. Basically, the PVDF membranes have medium rejection for cationic dyes such as MB [45], while another study reported that the rejection was good for both anionic and cationic dyes [46]. The natural pH of the MB solution is between 2–3.5 [47], but the AY17 solution has a natural pH of 5.28 [48], which is closer to neutral. The pH of both dye solutions influences the rejection mechanism, with the lower pH of the MB solution causing the molecule to have a higher positive charge. The positive charge of MB and the negative charge of the membrane surface are attracted to each other during filtration due to the presence of CA. As a result, the MB molecules are more tightly bound to the membrane surface and internal structure. This interaction had a high rejection value. In addition, because AY17 and the negative charge of the membrane surface repel each other, the AY17 molecules will be less attracted. Because the surface is insufficient to resist dye molecules, it causes a reduced rejection for AY17.

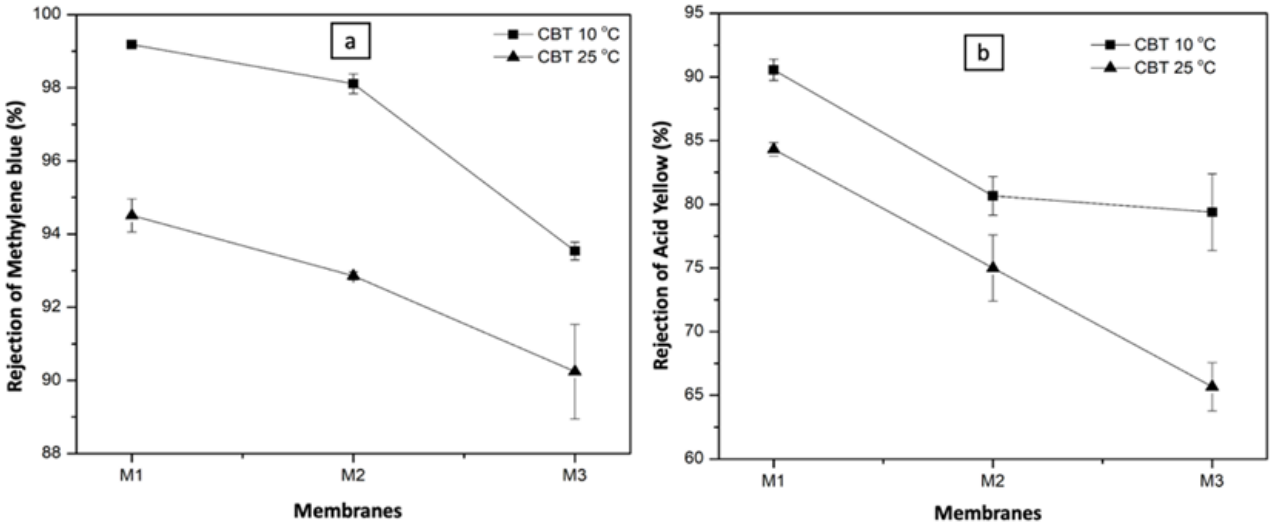

Figure 6 Effect of CBT on rejection of MB (a) and AY17 (b).

 DOI: 10.15826/chimtech.2024.11.2.01

In addition to the charge of the dye molecule, the size of the dye molecule also influences the rejection parameter. However, the charge interaction has a greater influence than the size of these dye molecules. Although larger pores have a higher probability of allowing dye molecules to pass through the membrane pores. However, Figure 6 shows a significant difference in rejection, with M3 absorbing less AY17 than MB. This is primarily due to a stronger membrane surface charge interaction with MB *vs.* AY17.

Flux recovery ratio is a metric used to evaluate the ability of a membrane to remove dye absorption during backwash. Varying the CBT results in a difference in the pore diameter of the membrane surface, as can be seen in Figure 4. Membranes with lower CBT load fewer dye molecules, resulting in a more effective backwash and higher FRR. Figure 7 shows that after filtering with AC instead of MB, the performance of the reused membranes was improved. All composite membranes maintained an FRR between 80 and 90% after AY17 filtration at a lower CBT. In addition, M2 and M3 demonstrated identical functionality at higher CBT (Figure 7b). However, after MB filtration, M3 showed the highest FRR at both higher and lower CBT, while the average FRR for the other membranes was below 80%.

Analysis of the time-dependent fluxes over 1.5 h of filtration is critical to confirming the % FRR data. Figure 8 shows that compaction (water flux) occurs during the first 30 min. Membrane backflushing with water continues for the next 90 min after the second 30 min of MB filtration. The dye flux was lower than the water flux for both CBTs. However, in most cases, the flux during water backwashing can be maintained at or near the final flux during the first 30 min of densification. However, the M3 membrane at higher CBT, which had a greater decrease in reverse flux than at lower CBT, presents a different picture. The M3 membrane at higher CBT exhibited a significantly higher drop in backflow than M3 at CBT 10 °C, as can be seen in the AY17 filtration shown in Figure 7. However, for both CBTs, the membrane backflow was often largely maintained or very slightly decreased.

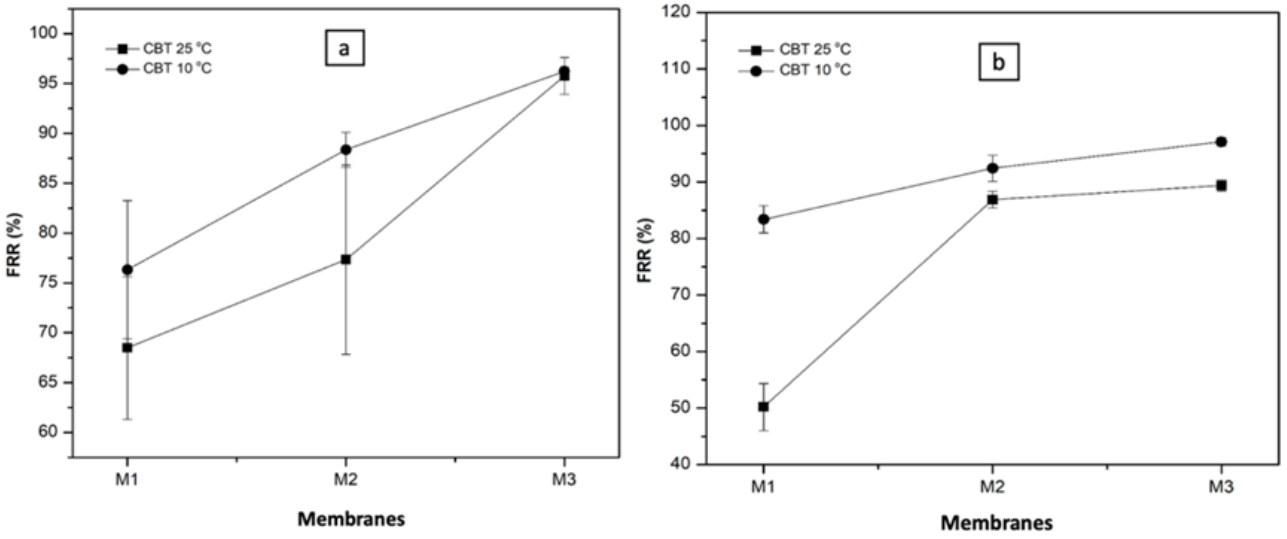

Figure 7 Effect of CBT on flux recovery ratio after filtration of (a) MB and (b) AY17.

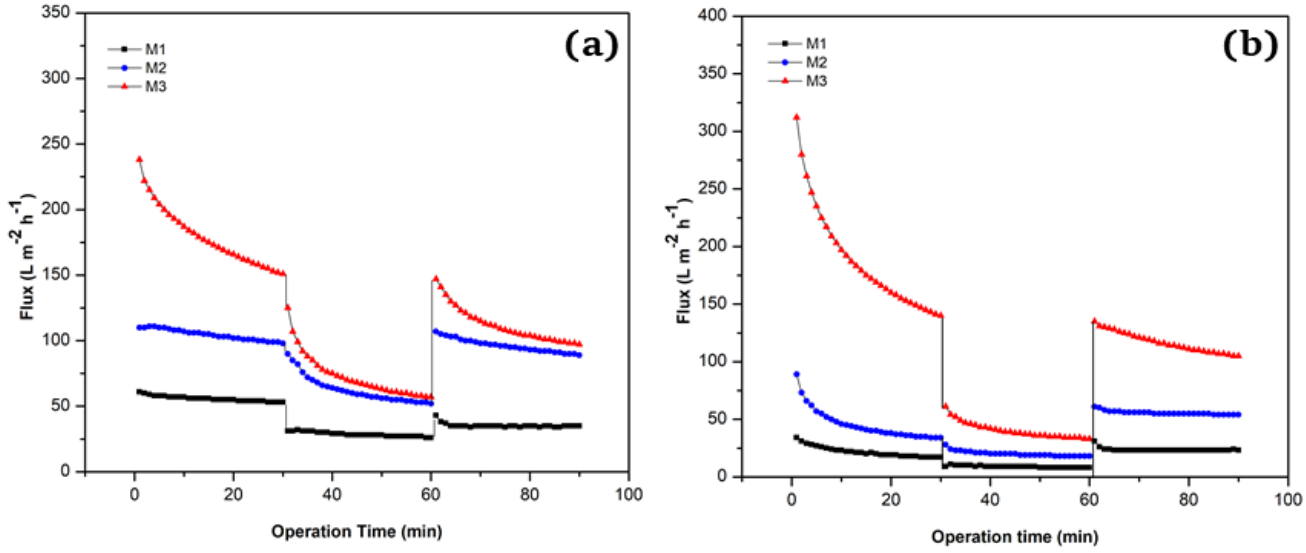

Figure 8 Effect of CBT 25 °C (a) and 10 °C (b) on time-dependent fluxes of MB filtration.

 DOI: 10.15826/chimtech.2024.11.2.01

Not only is rejection affected by the interaction of dye molecules with the membrane surfaces, but also the flux recovery ratio (%FRR). The higher FRR value indicates that the filtration performance of the membranes has been maintained. Figure 7 shows that AY17 typically has a higher FRR than MB. This conclusion is consistent with rejection; a higher rejection results in a lower FRR. Since the MB molecules were trapped both on the membrane surface and inside the structure, the strong bond between the MB molecules and the membrane structure will make the backwashing process more difficult. On the other hand, the performance of the membranes after AY17 filtration is better than that after MB filtration because of the weak interaction between AY17 molecules and membranes, which will facilitate backwashing. In addition, the FRR of MB and AY17 filtration is higher at lower CBT compared to higher CBT. Due to the less hydrophilic surface of the membranes created at lower CBT, more dye molecules aggregate on the surface, which facilitates backwashing.

The results validated the %FRR data shown in Figure 7 by the time-dependent fluxes shown in Figures 8 and 9. The time-dependent fluxes showed a similar trend because the AY17 filtration has a better FRR than the MB filtration. Figure 8 shows that overall, the water fluxes during the backwash process (60 to 90 min) did not decrease significantly compared to the water fluxes at 0 to 30 min. This result highlights how easily the membranes can be cleaned after AY17 filtration. Otherwise, the backwash fluxes were lower than the initial fluxes when the membranes were used for MB filtration (pure water fluxes). This is consistent with FRR data, which is generally lower than AY17 filtration. The effect of CBT on time-dependent fluxes is verified and explained in the FRR section below. The antifouling capabilities of PVDF/CA membranes can be determined based on time-dependent fluxes and FRR.

Measuring the fouling resistance of the membrane, expressed as reversible fouling and irreversible fouling, is important to determine the antifouling characteristics of the membrane. Figures 10 and 11 show that when the membrane was used for MB filtration compared to AY17, the overall fouling was greater. However, the reversible fouling of the lower CBT membrane is higher than that of the higher CBT membranes as shown in Figure 10. On the other hand, the irreversible fouling of the lower CBT membrane is less than that of the higher CBT membrane. As the amount of reversible fouling increases, the percentage of irreversible fouling continues to decrease. Figure 11 shows the same phenomenon, showing how reversible fouling continues to increase while irreversible fouling decreases. Although the membrane at lower CBT had more reversible fouling than the membrane at higher CBT. In addition to CBT, the antifouling properties are also affected by the concentration of CA added to the membranes [36]. Overall, the percentage of reduced fouling was found to be increase with the addition of CA.

Fouling is the term used to describe the phenomena where pores, both outside and inside the membrane structure, become clogged. When reversible fouling (R_r) is a higher percentage than irreversible fouling, membrane performance is favorable (R_{ir}). Physical treatment, such as backwashing, can eliminate reversible fouling. As a result, the higher percentage of FRR is accompanied by an increase in reversible fouling. In addition, for both MB and AY17 filtration, reversible fouling is proportionally higher at lower CBT than at higher CBT. This finding is still acceptable when compared to previous studies. Overall, the membranes cast at lower CBT have the higher percentage of reduced fouling. The comparative studies of antifouling properties between this recent study and others can be seen in Table 2.

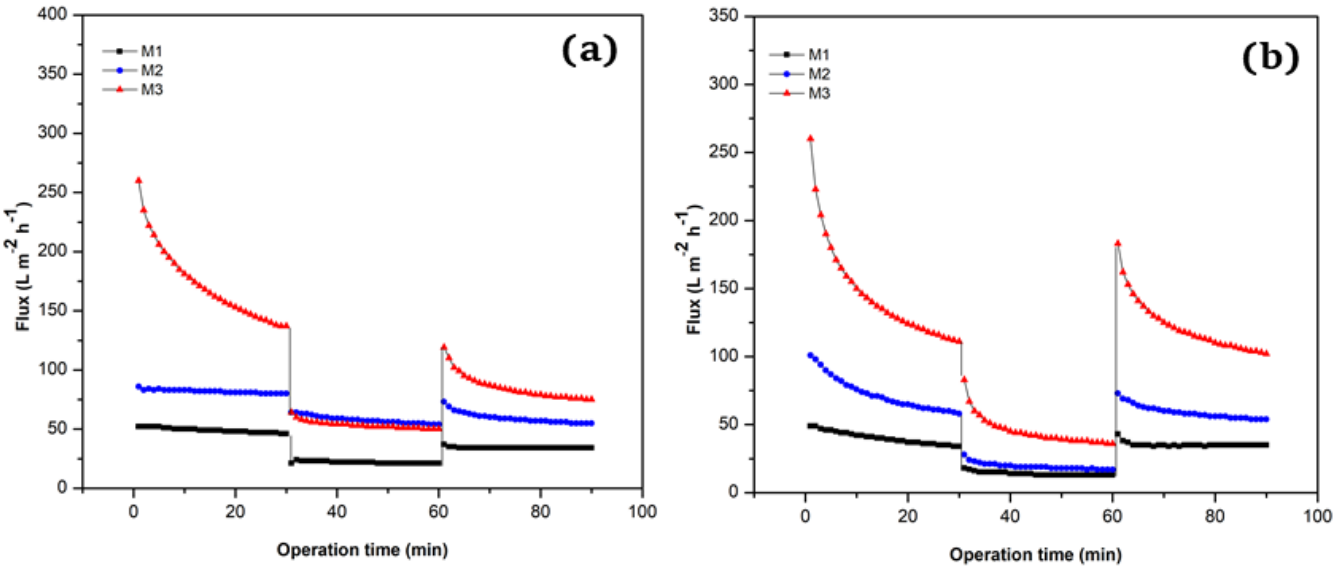

Figure 9 Effect of CBT 25 °C (a) and 10 °C (b) on time-dependent fluxes of AY17 filtration.

 DOI: 10.15826/chimtech.2024.11.2.01

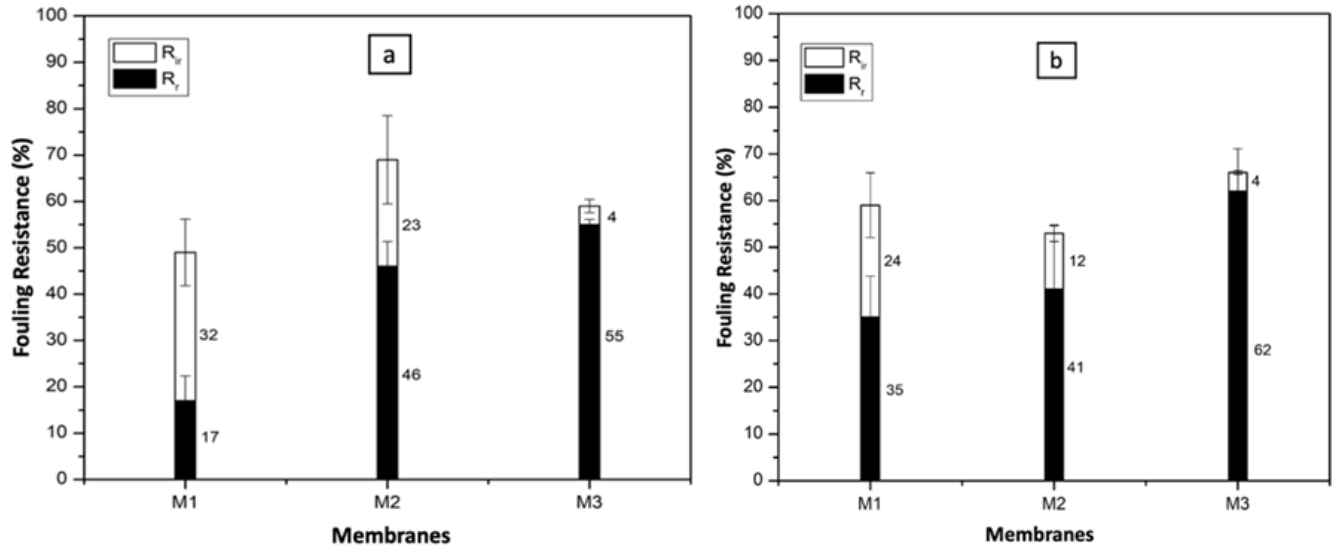

Figure 10 Effect of CBT 25 °C (a) and 10 °C (b) on fouling resistance of MB filtration.

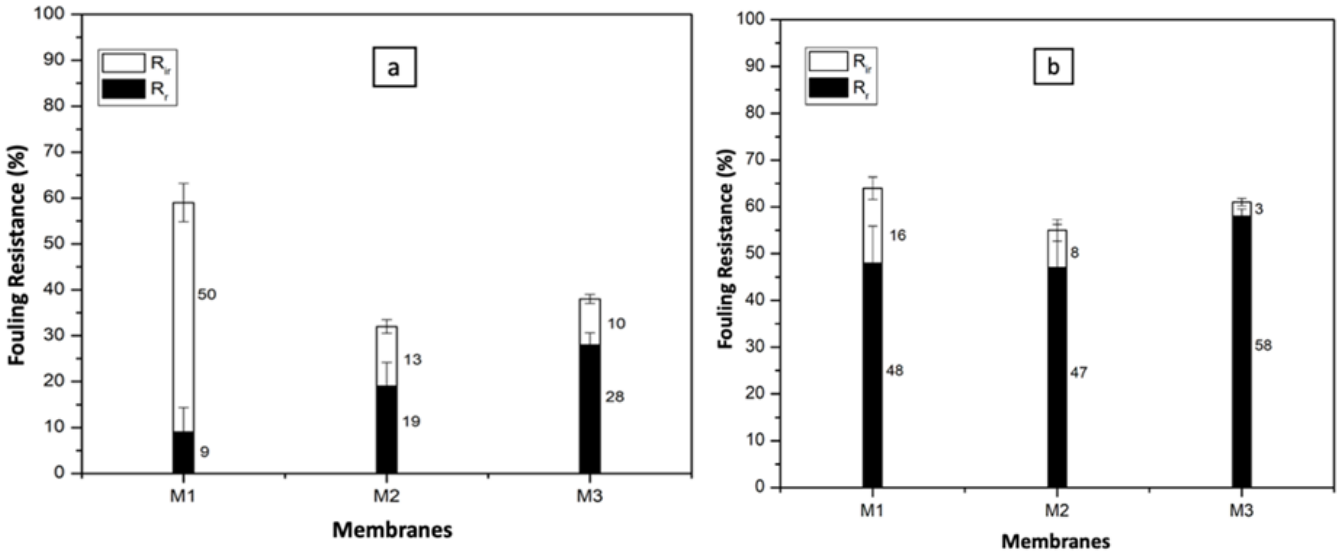

Figure 11 Effect of CBT 25 °C (a) and 10 °C (b) on fouling resistance of AY17 filtration.

Table 2 Comparison of fouling reduced percentage of membranes between this present work and previously published studies.

Membranes	CBT (°C)	Percentage of fouling reduced (%)	References
PVDF/CA	25	55	This study
PVDF/CA	10	62	This study
PVDF/CA	25	10	[49]
PVDF/CA	25	29	[50]
PVDF/CA/PA	25	75	[51]
PVDF-g-ZnS	25	58	[52]

4. Conclusions

Thermodynamically, the CBT variation results in a change of Gibbs free energy, which makes the membrane surface of CBT 25 °C more hydrophilic than CBT 10 °C. The SEM image shows that the membrane pore profiles of both CBT conditions are significantly different. Basically, membranes on CBT 10 with smaller pores have a higher rejection for both MB and AY. In addition to the pore size, the rejection is influenced by the charge interaction between the membrane and the dye load, which is more dominant than the dye molecular size, as evidenced by the higher MB rejection than AY. The pore profiles of the membranes have a significant impact on the microfiltration process, as the FRR of the membrane at CBT 10 °C is greater than that at CBT 25 °C. This is influenced by a more efficient backwashing process on membranes with smaller pores, as fewer dye molecules are loaded. This efficiency increases the number of reversible foulings. As a result, the CBT 25 °C membrane is more resistant to fouling than the CBT 10 °C membrane.

• Supplementary materials

No supplementary materials are available.

• Funding

This study had no external funding.

 DOI: 10.15826/chimtech.2024.11.2.01

• Acknowledgements

The authors acknowledge the support of Laboratory of Multidisciplinary of Universitas Islam Negeri Ar-Raniry and Laboratory of Physics Chemistry and Materials of Institut Teknologi Bandung.

• Author contributions

Conceptualization: M.R.
Data curation: M.R., R.F.I.R.
Formal analysis: M.R., R.F.I.R.
Investigation: M.R., R.F.I.R.
Methodology: M.R.
Resources: M.R., R.F.I.R.
Supervision: C.L.R.
Validation: R.F.I.R., C.L.R.
Visualization: M.R.
Writing – original draft: M.R.
Writing – review & editing: M.R., R.F.I.R., C.L.R.

• Conflict of interest

The authors declare no conflict of interest.

• Additional information

Author IDs:
Muhammad Reza, Scopus ID 58885515700;
Ratu Fazlia Inda Rahmayani, Scopus ID 57201675324;
Cynthia Linaya Radiman, Scopus ID 56524777900.

Websites:
Universitas Islam Negeri Ar-Raniry-Indonesia, https://ar-raniry.ac.id/;
Universitas Syiah Kuala-Indonesia, https://usk.ac.id/;
Institute Teknologi Bandung-Indonesia, https://www.itb.ac.id/.

• References

1. Saljoughi E, Amirilargani M, Mohammadi T. Effect of PEG additive and coagulation bath temperature on the morphology, permeability and thermal/chemical stability of asymmetric CA membranes. Desalination. 2010;262(1–3):72–78. doi:10.1016/j.desal.2010.05.046
2. Baker RW. Membrane technology and application second edition. California: John Wiley & Sons, Ltd; 2004.
3. Mulder M. Basic principles of membrane technology. Netherland: Kluwer Academic Publishers; 1996.
4. Feng C, Wang R, Zhang H, Shi L. Diverse morphologies of PVDF hollow fiber membranes and their performance analysis as gas/liquid contactors. J Appl Polym Sci. 2011;119(3):1259–1267. doi:10.1002/app.30250
5. Liu F, Hashim NA, Liu Y, Abed MRM, Li K. Progress in the production and modification of PVDF membranes. J Memb Sci. 2011;375(1–2):1–27. doi:10.1016/j.memsci.2011.03.014
6. Wang D, Li K, Teo WK. Preparation and characterization of polyvinylidene fluoride (PVDF) hollow fiber membranes. J Memb Sci. 1999;163(2):211–220. doi:10.1016/S0376-7388(99)00181-7
7. Baroña GNB, Cha BJ, Jung B. Negatively charged poly(vinylidene fluoride) microfiltration membranes by sulfonation. J Memb Sci. 2007;290(1–2):46–54. doi:10.1016/j.memsci.2006.12.013
8. Ma J, Wang Z, Pan M, Guo Y. A study on the multifunction of ferrous chloride in the formation of poly(vinylidene fluoride) ultrafiltration membranes. J Memb Sci. 2009;341(1–2):214–24. doi:10.1016/j.memsci.2009.06.008
9. Ong YK, Widjojo N, Chung TS. Fundamentals of semi-crystalline poly(vinylidene fluoride) membrane formation and its prospects for biofuel (ethanol and acetone) separation via pervaporation. J Memb Sci. 2011;378(1–2):149–162. doi:10.1016/j.memsci.2011.04.037
10. Hou D, Wang J, Qu D, Luan Z, Ren X. Fabrication and characterization of hydrophobic PVDF hollow fiber membranes for desalination through direct contact membrane distillation. Sep Purif Technol. 2009;69(1):78–86. doi:10.1016/j.seppur.2009.06.026
11. Yang X, Wang R, Shi L, Fane AG, Debowski M. Performance improvement of PVDF hollow fiber-based membrane distillation process. J Memb Sci. 2011;369(1–2):437–447. doi:10.1016/j.memsci.2010.12.020
12. Atchariyawut S, Feng C, Wang R, Jiraratananon R, Liang DT. Effect of membrane structure on mass-transfer in the membrane gas-liquid contacting process using microporous PVDF hollow fibers. J Memb Sci. 2006;285(1–2):272–281. doi:10.1016/j.memsci.2006.08.029
13. Peng J, Su Y, Chen W, Shi Q, Jiang Z. Effects of coagulation bath temperature on the separation performance and antifouling property of poly(ether sulfone) ultrafiltration membranes. Ind Eng Chem Res. 2010;49(10):4858–4864. doi:10.1021/ie9018963
14. Wang D, Li K, Teo WK. Porous PVDF asymmetric hollow fiber membranes prepared with the use of small molecular additives. J Memb Sci. 2000;178(1–2):13–23. doi:10.1016/S0376-7388(00)00460-9
15. Yuan GL, Xu ZL, Wei YM. Characterization of PVDF-PFSA hollow fiber UF blend membrane with low-molecular weight cut-off. Sep Purif Technol. 2009;69(2):141–148. doi:10.1016/j.seppur.2009.07.011
16. Conesa A, Gumí T, Palet C. Membrane thickness and preparation temperature as key parameters for controlling the macrovoid structure of chiral activated membranes (CAM). J Memb Sci. 2007;287(1):29–40. doi:10.1016/j.memsci.2006.10.006
17. Kumar M, Ulbricht M. Novel ultrafiltration membranes with adjustable charge density based on sulfonated poly(arylene ether sulfone) block copolymers and their tunable protein separation performance. Polymer. 2014;55(1):354–365. doi:10.1016/j.polymer.2013.09.003
18. Torrestiana-Sanchez B, Ortiz-Basurto RI, Brito-De E, Fuente L. Effect of nonsolvents on properties of spinning solutions and polyethersulfone hollow fber ultrafiltration membranes. J Memb Sci. 1999;152:19–28. doi:10.1016/S0376-7388(98)00172-0
19. Cheng LP. Effect of temperature on the formation of microporous PVDF membranes by precipitation from 1-Octanol/DMF/PVDF and water/ DMF/PVDF systems. Macromolecules. 1999;32(20):6668–6674. doi:10.1021/ma9904181
20. Saljoughi E, Amirilargani M, Mohammadi T. Effect of poly(vinyl pyrrolidone) concentration and coagulation bath temperature on the morphology, permeability, and thermal stability of asymmetric cellulose acetate membranes. J Appl Polym Sci. 2009;111(5):2537–2544. doi:10.1002/app.29354
21. Wang GJ, Chu LY, Zhou MY, Chen WM. Effects of preparation conditions on the microstructure of porous microcapsule membranes with straight open pores. J Memb Sci. 2006;284(1–2):301–312. doi:10.1016/j.memsci.2006.07.048
22. Wang X, Zhang L, Sun D, An Q, Chen H. Effect of coagulation bath temperature on formation mechanism of poly(vinylidene fluoride) membrane. J Appl Polym Sci. 2008;110(3):1656–1663. doi:10.1002/app.28169

 DOI: 10.15826/chimtech.2024.11.2.01

23. Shin SJ, Kim JP, Kim HJ, Jeon JH, Min BR. Preparation and characterization of polyethersulfone microfiltration membranes by a 2-methoxyethanol additive. Desalination. 2005;186(1–3):1–10. doi:10.1016/j.desal.2005.03.092
24. Hossein Razzaghi M, Safekordi A, Tavakolmoghadam M, Rekabdar F, Hemmati M. Morphological and separation performance study of PVDF/CA blend membranes. J Memb Sci. 2014;470:547–557. doi:10.1016/j.memsci.2014.07.026
25. Reza M, Pramono E, Radiman CL. Improving Separation Performance of PVDF Ultrafiltration Membranes by Blending with Cellulose Acetate. J Chem Chem Eng. 2023;42(3):1017–29. doi:10.30492/ijcce.2022.550394.5221
26. 26. Loh CH, Wang R. Effects of additives and coagulant temperature on fabrication of high performance PVDF/Pluronic F127 blend hollow fiber membranes via nonsolvent induced phase separation. Chin J Chem Eng. 2012;20(1):71–79. doi:10.1016/S1004-9541(12)60365-6
27. Saraswathi MSSA, Rana D, Alwarappan S, Gowrishankar S, Vijayakumar P, Nagendran A. Polydopamine layered poly (ether imide) ultrafiltration membranes tailored with silver nanoparticles designed for better permeability, selectivity and antifouling. J Ind Eng Chem. 2019;76:141–149. doi:10.1016/j.jiec.2019.03.014
28. Miller DJ, Kasemset S, Paul DR, Freeman BD. Comparison of membrane fouling at constant flux and constant transmembrane pressure conditions. J Memb Sci. 2014;454:505–515. doi:10.1016/j.memsci.2013.12.027
29. Vadivelan V, Vasanth Kumar K. Equilibrium, kinetics, mechanism, and process design for the sorption of methylene blue onto rice husk. J Colloid Interface Sci. 2005;286(1):90–100. doi:10.1016/j.jcis.2005.01.007
30. Nair VR, Shetty Kodialbail V. Floating bed reactor for visible light induced photocatalytic degradation of Acid Yellow 17 using polyaniline-TiO_2 nanocomposites immobilized on polystyrene cubes. Environ Sci Pollut Res Int. 2020;27(13):14441–14453. doi:10.1007/s11356-020-07959-2
31. Jayalakshmi A, Rajesh S, Mohan D. Fouling propensity and separation efficiency of epoxidated polyethersulfone incorporated cellulose acetate ultrafiltration membrane in the retention of proteins. Appl Surf Sci. 2012;258(24):9770–9781. doi:10.1016/j.apsusc.2012.06.028
32. Lapointe JF, Gauthier SF, Pouliot Y, Bouchard C. Characterization of interactions between β-lactoglobulin tryptic peptides and a nanofiltration membrane: Impact on the surface membrane properties as determined by contact angle measurements. J Memb Sci. 2005;261(1–2):36–48. doi:10.1016/j.memsci.2005.03.030
33. Khayet M, Cojocaru C, García-Payo MC. Experimental design and optimization of asymmetric flat-sheet membranes prepared for direct contact membrane distillation. J Memb Sci. 2010;351(1–2):234–245. doi:10.1016/j.memsci.2010.01.057
34. Wongchitphimon S, Wang R, Jiraratananon R, Shi L, Loh CH. Effect of polyethylene glycol (PEG) as an additive on the fabrication of polyvinylidene fluoride-co-hexafluoropropylene (PVDF-HFP) asymmetric microporous hollow fiber membranes. J Memb Sci. 2011;369(1–2):329–338. doi:10.1016/j.memsci.2010.12.008
35. Yeow ML, Liu YT, Li K. Isothermal Phase Diagrams and Phase-Inversion Behavior of Poly(vinylidene fluoride)/Solvents/Additives/Water Systems. J Appl Polym Sci. 2003;90:2150–2155. doi:10.1002/app.12846
36. Reza M, Pramono E, Cyntia LR. Improving Separation Performance of PVDF Ultrafiltration Membranes by Blending with Cellulose Acetate. J Chem Chem Eng. 2023;42(3):1017–1029. doi:10.30492/ijcce.2022.550394.5221
37. Li J, Ren LF, Zhou HS, Yang J, Shao J, He Y. Fabrication of superhydrophobic PDTS-ZnO-PVDF membrane and its anti-wetting analysis in direct contact membrane distillation (DCMD) applications. J Memb Sci. 2021;620. doi:10.1016/j.memsci.2020.118924
38. Lafuma A, Quéré D. Superhydrophobic states. Nat Mater. 2003;2(7):457–460. https://www.nature.com/articles/nmat924
39. Curcio E, Fontananova E, Di Profio G, Drioli E. Influence of the structural properties of poly(vinylidene fluoride) membranes on the heterogeneous nucleation rate of protein crystals. J Phys Chem B. 2006;110(25):12438–12445. doi:10.1021/jp061531y
40. Umam K, Sagita F, Pramono E, Ledyastuti M, Kadja GTM, Radiman CL. Polyvinylidenefluoride (PVDF)/surface functionalized-mordenite mixed matrix membrane for congo red dyes removal: Effect of types of organosilane. JCIS Open. 2023;11. doi:10.1016/j.jciso.2023.100093
41. Huang FL, Wang QQ, Wei QF, Gao WD, Shou HY, Jiang SD. Dynamic wettability and contact angles of poly(vinylidene fluoride) nanofiber membranes grafted with acrylic acid. Express Polym Lett. 2010;4(9):551–558. doi:10.3144/expresspolymlett.2010.69
42. Hebbar RS, Isloor AM, Ismail AF. Contact Angle Measurements. In: Membrane Characterization. Elsevier Inc. 2017; 219–255. doi:10.1016/B978-0-444-63776-5.00012-7
43. Chen Y, Tian M, Li X, Wang Y, An AK, Fang J, et al. Anti-wetting behavior of negatively charged superhydrophobic PVDF membranes in direct contact membrane distillation of emulsified wastewaters. J Memb Sci. 2017;535:230–238. doi:10.1016/j.memsci.2017.04.040
44. Breite D, Went M, Prager A, Schulze A. Tailoring membrane surface charges: A novel study on electrostatic interactions during membrane fouling. Polymers. 2015;7(10):2017–30. doi:10.3390/polym7101497
45. Tran TT Van, Kumar SR, Lue SJ. Separation mechanisms of binary dye mixtures using a PVDF ultrafiltration membrane: Donnan effect and intermolecular interaction. J Memb Sci. 2019;575:38–49. doi:10.1016/j.memsci.2018.12.070
46. Ghaffar A, Zhang L, Zhu X, Chen B. Porous PVdF/GO nanofibrous membranes for selective separation and recycling of charged organic dyes from water. Environ Sci Technol. 2018;52(7):4265–74. doi:10.1021/acs.est.7b06081
47. Oladoye PO, Ajiboye TO, Omotola EO, Oyewola OJ. Methylene blue dye: Toxicity and potential elimination technology from wastewater. Res Eng. 2022;16. doi:10.1016/j.rineng.2022.100678
48. Adar E. Removal of Acid Yellow 17 from textile wastewater by adsorption and heterogeneous persulfate oxidation. Int J Environ Sci Technol. 2021;18(2):483–498. doi:10.1007/s13762-020-02986-5
49. Razzaghi MH, Tavakolmoghadam M, Rekabdar F, Oveisi F. Investigation of the effect of coagulation bath composition on PVDF/CA membrane by evaluating critical flux and antifouling properties in lab-scale submerged MBR. Water Environ J. 2018;32(3):366–376. doi:10.1111/wej.12334
50. Hossein Razzaghi M, Safekordi A, Tavakolmoghadam M, Rekabdar F, Hemmati M. Morphological and separation performance study of PVDF/CA blend membranes. J Memb Sci. 2014;470:547–57. doi:10.1016/j.memsci.2014.07.026
51. Duong PHH, Nunes SP, Chung TS. Dual-skinned polyamide/poly(vinylidene fluoride)/cellulose acetate membranes with embedded woven. J Memb Sci. 2016;520:840–849. doi:10.1016/j.memsci.2016.08.047
52. Du J, Li N, Tian Y, Zhang J, Zuo W. Preparation of PVDF membrane blended with graphene oxide-zinc sulfide (GO-ZnS) nanocomposite for improving the anti-fouling property. J Photochem Photobiol A Chem. 2020;400. doi:10.1016/j.jphotochem.2020.112694